Contribution from the Departments of Chemistry, The Pennsylvania State University, University Park, Pennsylvania 16802, and University of Nebraska, Lincoln, Nebraska 68588, and from Crystalytics Company, Lincoln, Nebraska 68501

Reaction of $H_2FeRu_3(CO)_{13}$ with Tertiary Phosphines and Phosphites. Influence of Ligand Size and Basicity on Substitution Site Preference. Crystal and Molecular Structure of $H_2FeRu_3(CO)_{12}(PMe_2Ph)$

JOSEPH R. FOX,[1a] WAYNE L. GLADFELTER,[1a] TIMOTHY G. WOOD,[1a] JOHN A. SMEGAL,[1a] THOMAS K. FOREMAN,[1a] GREGORY L. GEOFFROY,*[1a] IRAQ TAVANAIEPOUR,[1b] V. W. DAY,[1b] and C. S. DAY[1c]

Received January 27, 1981

Reaction of the mixed-metal cluster $H_2FeRu_3(CO)_{13}$ with a series of tertiary phosphines and phosphites (L = PPh_3, PPh_2Me, $PPhMe_2$, $PPhEt_2$, $P(OMe)_3$, $P(OEt)_3$, $P(OEt)_2Ph$, PMe_3, $P(i\text{-}Pr)_3$) leads to the formation of substituted clusters of the form $H_2FeRu_3(CO)_{13-n}L_n$ (n = 1, 2) in 20–30% yield. Small quantities of trisubstituted clusters have also been isolated from the reactions employing PPh_3, $P(OMe)_3$, and $P(OEt)_3$. The infrared spectra of the substituted clusters are similar to that of $H_2FeRu_3(CO)_{13}$ and indicate that no severe structural changes occur in the cluster upon substitution. Detailed ^{31}P and ^1H NMR studies show that the monosubstituted clusters can exist in two isomeric forms of C_s and C_1 symmetries. The ratio of these two isomers for a given phosphorus donor ligand is dependent on *both* the ligand size and basicity. Large ligands give exclusively the C_s isomer. With small ligands, basicity becomes the controlling factor with the more basic ligands preferring the C_1 isomer. Kinetic measurements indicate that the substitution reaction of $H_2FeRu_3(CO)_{13}$ with PPh_3 proceeds by a first-order, [PPh_3]-independent path, presumably involving CO dissociation from $H_2FeRu_3(CO)_{13}$ in the rate-determining step, with activation parameters $\Delta H^{\circ\ddagger} = 25.3 \pm 0.9$ kcal/mol and $\Delta S^{\circ\ddagger} = 4.9 \pm 3.1$ cal/(mol K). The structure of the C_s isomer of $H_2FeRu_3(CO)_{12}(PMe_2Ph)$ has been determined by X-ray diffraction. It crystallizes in the space group $P\bar{1}$-C_i^1 (No. 2) with a = 9.958 (4) Å, b = 9.970 (3) Å, c = 14.705 Å, α = 87.36 (2)°, β = 104.88 (3)°, and γ = 103.76 (3)° with Z = 2. The structure was refined to R_1 = 0.034 and R_2 = 0.035 for 5490 independent reflections having $I > 3.0\sigma(I)$. The overall geometry of $H_2FeRu_3(CO)_{12}(PMe_2Ph)$ is similar to that of the parent $H_2FeRu_3(CO)_{13}$ cluster, implying that little distortion occurs upon substitution. The hydrides were located and refined in the $H_2FeRu_3(CO)_{12}(PMe_2Ph)$ structure and bridge two of the three Ru–Ru bonds in accord with the suggestion made earlier for $H_2FeRu_3(CO)_{13}$ on the basis of bond length arguments. The phosphorus atom is attached to the Ru atom that is also ligated by both hydrides and lies 2.11 Å below the Ru_3 plane.

A variety of new and extremely interesting cluster compounds have been prepared and characterized in recent years,[2] and considerable progress has been made in developing better methods for directing the synthesis of particularly desired clusters.[3-7] However, far fewer studies have focused on the reactivity features of these compounds even though it is essential that their basic reactivity patterns be well understood if cluster compounds are to be employed as catalysts or used in synthetic transformations.

Mixed-metal clusters are ideally suited for reactivity studies since the asymmetry which is inherent within their framework can allow definition of reactivity sites and mechanism. Recognizing this, we have undertaken a series of reactivity studies of mixed-metal clusters, with an initial focus on $H_2FeRu_3(CO)_{13}$. It has been our intent to examine thoroughly the reactions of this particular compound in order to understand fully its reactivity features. This particular cluster was chosen because it is easily prepared in high yield (>50%) and in sufficient quantities to allow these studies to be conducted.[3] Furthermore, $H_2FeRu_3(CO)_{13}$ is one of the most active clusters for catalyzing the water-gas shift reaction,[8] and thus these studies should provide important insight into the mechanism of this catalysis.

We have previously reported the fluxional properties of $H_2FeRu_3(CO)_{13}$[9] and also its fragmentation reaction with CO, eq 1.[10] Herein we describe the reactions of $H_2FeRu_3(CO)_{13}$

$$H_2FeRu_3(CO)_{13} + CO \rightarrow Ru_3(CO)_{12} + Fe(CO)_5 + H_2 \quad (1)$$

with a series of tertiary phosphines and phosphites which give substituted clusters of the form $H_2FeRu_3(CO)_{13-n}L_n$ (n = 1–3). Through detailed ^1H NMR and IR studies, and a complete structural characterization of one of the isomers by X-ray diffraction, the specific substitution sites in these derivatives have been determined and the choice of substitution site has been correlated with the size and basicity of the specific ligand. The fluxional properties of these substituted derivatives, in which the structural isomers interconvert, and the reactions of $H_2FeRu_3(CO)_{13}$ with a series of alkynes are discussed in the following two articles.[11,12]

(1) (a) The Pennsylvania State University. (b) University of Nebraska. (c) Crystalytics Co.
(2) Recent reviews include: (a) Chini, P.; Longoni, G.; Albano, V. G. *Adv. Organomet. Chem.* **1976**, *14*, 285. (b) Chini, P.; Heaton, B. T. *Top. Curr. Chem.* **1977**, *71*, 1. (c) Band, E.; Muetterties, E. L. *Chem. Rev.* **1978**, *78*, 639. (d) Gladfelter, W. L.; Geoffroy, G. L. *Adv. Organomet. Chem.* **1980**, *18*, 207. (e) Johnson, B. F. G.; Benfield, R. E. *Top. Stereochem.* **1981**, *12*, 253. (f) Humphries, A. P.; Kaesz, H. D. *Prog. Inorg. Chem.* **1978**, *25*, 145.
(3) Geoffroy, G. L.; Gladfelter, W. L. *J. Am. Chem. Soc.* **1977**, *99*, 7565.
(4) Steinhardt, P. C.; Gladfelter, W. L.; Harley, A. D.; Fox, J. R.; Geoffroy, G. L. *Inorg. Chem.* **1980**, *19*, 332.
(5) Richter, F.; Vahrenkamp, H. *Angew. Chem., Int. Ed. Engl.* **1978**, *17*, 864; **1979**, *18*, 531.
(6) (a) Shapley, J. R.; Pearson, G. A.; Tachikawa, M.; Schmidt, G.; Churchill, M. R.; Hollander, F. J. *J. Am. Chem. Soc.* **1977**, *99*, 8064. (b) Churchill, M. R.; Hollander, F. J.; Shapley, J. R.; Foose, D. S. *J. Chem. Soc., Chem. Commun.* **1978**, 534.
(7) (a) Ashworth, T. V.; Berry, M.; Howard, J. A. K.; Laguna, N.; Stone, F. G. A. *J. Chem. Soc., Chem. Commun.* **1979**, 45. (b) Ashworth, T. V.; Howard, J. A. K.; Stone, F. G. A. *Ibid.* **1979**, 42. (c) Farrugia, L. J.; Howard, J. A. K.; Mitrprachachon, P.; Spencer, J. L.; Stone, F. G. A.; Woodward, P. *Ibid.* **1978**, 260.
(8) (a) Laine, R. M.; Rinker, R. G.; Ford, P. C. *J. Am. Chem. Soc.* **1977**, *99*, 252. (b) Ford, P. C.; Rinker, R. G.; Ungermann, C.; Laine, R. M.; Landis, V.; Moya, S. A. *Ibid.* **1978**, *100*, 4595. (c) Ungermann, C.; Landis, V.; Moya, S. A.; Cohen, H.; Walker, H.; Pearson, R. G.; Rinker, R. G.; Ford, P. C. *Ibid.* **1979**, *101*, 5922.
(9) (a) Geoffroy, G. L.; Gladfelter, W. L. *J. Am. Chem. Soc.* **1977**, *99*, 6775. (b) Gladfelter, W. L.; Geoffroy, G. L. *Inorg. Chem.* **1980**, *19*, 2579.
(10) Fox, J. R.; Gladfelter, W. L.; Geoffroy, G. L. *Inorg. Chem.* **1980**, *19*, 2574.
(11) Gladfelter, W. L.; Fox, J. R.; Smegal, J. A.; Wood, T. G.; Geoffroy, G. L. *Inorg. Chem.*, companion paper in this issue.
(12) Fox, J. R.; Gladfelter, W. L.; Geoffroy, G. L.; Day, V. W.; Abdel-Meguid, S.; Tavanaiepour, I. *Inorg. Chem.*, companion paper in this issue.

0020-1669/81/1320-3214$01.25/0

Table I. Experimental Details for the Reaction of $H_2FeRu_3(CO)_{13}$ with PR_3

PR_3	solvent	temp, °C	time, min	chromatographic solvent	products	yield, %	anal.	%C	%H
PPh_3	heptane	70	30	5:1 hexane/CH_2Cl_2	$H_2FeRu_3(CO)_{12}(PPh_3)$	33	calcd	37.55	1.79
							found	36.96	1.71
					$H_2FeRu_3(CO)_{11}(PPh_3)_2$	25	calcd	47.29	2.70
							found	47.32	2.90
					$H_2FeRu_3(CO)_{10}(PPh_3)_3$	trace			
$PMePh_2$	CH_2Cl_2	40	150	2:1 benzene/hexane	$H_2FeRu_3(CO)_{12}(PMePh_2)$	41	calcd	33.46	1.69
							found	33.41	1.75
PMe_2Ph	CH_2Cl_2	25	120	3:1 hexane/benzene	$H_2FeRu_3(CO)_{12}(PMe_2Ph)$	33	calcd	28.69	1.57
							found	28.69	1.60
PMe_3	hexane	25	60	4:1 hexane/CH_2Cl_2	$H_2FeRu_3(CO)_{12}PMe_3$	10	calcd	23.30	1.43
							found	23.24	1.55
					$H_2FeRu_3(CO)_{11}(PMe_3)_2$	5	calcd	24.86	2.45
							found	26.86	3.28
$P(i\text{-}Pr)_3$	CH_2Cl_2	40	120	4:1 hexane/CH_2Cl_2	$H_2FeRu_3(CO)_{12}(P(i\text{-}Pr)_3)$	18	calcd	29.42	2.70
							found	29.24	2.72
PEt_2Ph	CH_2Cl_2	25	60	3:1 hexane/benzene	$H_2FeRu_3(CO)_{12}PEt_2Ph$	40	calcd	30.60	1.98
							found	30.45	2.04
					$H_2FeRu_3(CO)_{11}(PEt_2Ph)_2$	...	calcd	37.15	3.22
							found	37.03	3.26
$P(OEt)_2Ph$	CH_2Cl_2	40	180	10:1 hexane/benzene	$H_2FeRu_3(CO)_{12}(P(OEt)_2Ph)$	23	calcd	29.52	1.91
							found	29.65	2.85
$P(OMe)_3$	hexane	50	45	4:1 hexane/CH_2Cl_2	$H_2FeRu_3(CO)_{12}(P(OMe)_3)$	41	calcd	21.94	1.35
							found	22.20	1.50
					$H_2FeRu_3(CO)_{12}(P(OMe)_3)_2$	36	calcd	22.26	2.20
							found	22.49	2.43
					$H_2FeRu_3(CO)_{10}(P(OMe)_3)_3$	trace			
$P(OEt)_3$	hexane	50	150	4:1 hexane/CH_2Cl_2	$H_2FeRu_3(CO)_{12}(P(OEt)_3)$	28	calcd	25.04	1.98
							found	25.08	2.02
					$H_2FeRu_3(CO)_{11}(P(OEt)_3)_2$	18	calcd	27.58	3.22
							found	30.71	3.85?
					$H_2FeRu_3(CO)_{10}(P(OEt)_3)_3$	trace			

Experimental Section

The phosphines PMe_3, PMe_2Ph, $PMePh_2$, PEt_2Ph, PPh_3, and $P(i\text{-}Pr)_3$ were purchased from Strem Chemical Co. and were used as received. $P(OMe)_3$ and $P(OEt)_3$ were obtained from Aldrich Chemical Co. and were distilled under N_2 immediately prior to use. $H_2FeRu_3(CO)_{13}$[3] and $P(OEt)_2Ph$[13] were prepared according to literature procedures. All solvents were dried over CaH_2 or $LiAlH_4$ prior to use, and all reactions were carried out under an N_2 atmosphere unless otherwise specified. Progress of the reactions was monitored by thin-layer chromatography or by high-pressure analytical liquid chromatography. Elemental analyses were performed by Galbraith Laboratories, Knoxville, TN.

General Synthetic Procedure. Specific details concerning the solvents employed, time, temperature, products, and yields of the reactions of $H_2FeRu_3(CO)_{13}$ with the various phosphines and phosphites are given in Table I. In general, a solution of $H_2FeRu_3(CO)_{13}$ and the appropriate ligand in slight excess of a 1:1 ratio was heated until chromatographic analysis indicated that most of the $H_2FeRu_3(CO)_{13}$ had reacted. The solution was then cooled, concentrated, and chromatographed on silica gel by using the previously described low-pressure liquid chromatography apparatus.[3] Yields are relative to the amount of reacted $H_2FeRu_3(CO)_{13}$.

Kinetics of the Reaction of $H_2FeRu_3(CO)_{13}$ with PPh_3. For each kinetic experiment, a 5-mL aliquot of a standard hexane solution of $H_2FeRu_3(CO)_{13}$ (1.0×10^{-3} M) was placed in a 25-mL Schlenk flask. The appropriate amount of solid PPh_3 (2–100-fold excess) and 10 μL of toluene as an internal standard were added to the solution. The Schlenk flask was sealed with a serum cap and the solution degassed via three freeze–pump–thaw cycles and placed under an N_2 or a CO atmosphere. The Schlenk flask was immersed in a temperature-controlled water bath, and 20-μL samples were removed periodically via an airtight syringe and analyzed by high-pressure liquid chromatography. The analytical liquid chromatograph consists of a Waters Associates M-6000A pump and 25-cm μ-Porasil chromatography column coupled with a Du Pont Model 830 detector, injector, and recorder. Hexane was the eluting solvent at a flow rate of 2.0 mL/min. Plots of $\ln\{[FeRu_3][toluene]_0/[FeRu_3]_0[toluene]\}$ vs. time were obtained from measurements of the areas under the toluene and $H_2FeRu_3(CO)_{13}$ peaks in each chromatogram and were linear to 80% completion. The errors in the activation parameters are reported as 95% confidence limits, $\lambda = ts$, where s is the standard error, t is the appropriate correction factor for $(N-2)$ degrees of freedom, and N is the number of measurements.[14] For the data reported herein, $N = 6$ and $t = 3.5$.

Table II. Data for X-ray Diffraction Study of $H_2FeRu_3(CO)_{12}(PMe_2Ph)$

Crystal Parameters	
cryst system: triclinic	$a = 9.958$ (4) Å
space group: $P\bar{1}$-C_i^1 (No. 2)	$b = 9.970$ (3) Å
$V = 1370.3$ (3) Å^3	$c = 14.705$ (4) Å
$Z = 2$	$\alpha = 87.36$ (2)°
calcd density = 2.02 g cm^{-3}	$\beta = 104.83$ (3)°
temp = 20 ± 1 °C	$\gamma = 103.76$ (3)°
cryst dimens: 0.25 × 0.25 × 0.29 mm	abs coeff: 22.3 cm^{-1}

Measurement of Intensity Data
diffractometer: four-circle Nicolet autodiffractometer
radiation: Mo Kα (λ 0.710 73 Å)
monochromator: graphite crystal
scan method: ω; fixed background; bkgd/scan time = 1.0
scan speed fixed: 3.0° min^{-1}, $2\theta < 43°$; 2.0° min^{-1}, $43° < 2\theta < 55°$; 1.0° min^{-1}, $55° < 2\theta < 63.4°$
scan range: 1.0°
takeoff angle: 4°
std reflctns = 6/300, no variations
data limits: $0° < 2\theta < 63.4°$
unique data: 9270
nonzero data: 5490 ($I > 3\sigma(I)$)
no. of variables: 386
goodness of fit: 1.31

Spectral Measurements. IR spectra were recorded in either CH_2Cl_2 or hexane solution on a Perkin-Elmer 580 grating infrared spectrophotometer using 0.5-mm NaCl solution IR cells. Electron-impact

(13) Rabinowitz, R.; Pellon, J. *J. Org. Chem.* **1961**, *26*, 4623.

(14) Draper, N. R.; Smith, H. "Applied Regression Analysis"; Wiley: New York, 1966; pp 18–24.

Table III. Atomic Coordinates for Nonhydrogen Atoms in Crystalline $H_2FeRu_3(CO)_{12}(PMe_2Ph)$[a]

atom type[b]	fractional coordinates		
	x	*y*	*z*
Ru_1	0.006 84 (4)	0.265 31 (3)	0.664 71 (2)
Ru_2	0.090 98 (5)	0.331 90 (4)	0.864 99 (3)
Ru_3	0.132 92 (4)	0.083 34 (4)	0.805 19 (3)
Fe	0.285 12 (7)	0.329 81 (7)	0.764 60 (5)
P	−0.240 18 (13)	0.188 76 (13)	0.612 72 (9)
O_{b1}	0.303 97 (57)	0.609 10 (41)	0.825 02 (41)
O_{b2}	0.315 10 (45)	0.107 79 (43)	0.654 96 (33)
O_{11}	−0.001 15 (61)	0.553 31 (40)	0.596 28 (31)
O_{12}	0.048 64 (51)	0.164 49 (47)	0.485 63 (28)
O_{21}	−0.154 54 (51)	0.182 08 (55)	0.944 77 (34)
O_{22}	0.009 21 (76)	0.601 39 (57)	0.887 71 (43)
O_{23}	0.317 56 (60)	0.345 97 (55)	1.050 71 (32)
O_{31}	−0.093 75 (48)	−0.083 78 (46)	0.896 54 (31)
O_{32}	0.142 84 (65)	−0.184 83 (47)	0.717 58 (36)
O_{33}	0.372 61 (51)	0.071 74 (55)	0.978 89 (33)
O_{41}	0.346 35 (59)	0.470 81 (54)	0.596 98 (35)
O_{42}	0.577 81 (50)	0.351 72 (56)	0.877 90 (42)
C_{b1}	0.270 71 (59)	0.490 70 (54)	0.810 97 (42)
C_{b2}	0.281 19 (51)	0.169 09 (53)	0.707 62 (40)
C_{11}	0.003 82 (59)	0.444 46 (50)	0.621 02 (33)
C_{12}	0.034 68 (55)	0.204 73 (50)	0.552 61 (34)
C_{21}	−0.060 32 (64)	0.232 17 (60)	0.914 31 (36)
C_{22}	0.042 88 (76)	0.503 16 (65)	0.880 62 (41)
C_{23}	0.232 07 (70)	0.338 94 (59)	0.982 05 (39)
C_{31}	−0.010 42 (57)	−0.015 37 (55)	0.863 43 (36)
C_{32}	0.139 52 (68)	−0.085 50 (55)	0.749 14 (40)
C_{33}	0.282 95 (61)	0.076 71 (60)	0.914 95 (41)
C_{41}	0.320 39 (64)	0.417 03 (61)	0.662 27 (45)
C_{42}	0.462 89 (66)	0.343 54 (62)	0.837 05 (46)
C_1	−0.340 70 (88)	0.303 15 (87)	0.639 52 (75)
C_2	−0.309 28 (83)	0.168 80 (94)	0.486 13 (46)
C_3	−0.311 60 (49)	0.020 67 (54)	0.657 34 (35)
C_4	−0.383 80 (68)	0.004 02 (83)	0.727 86 (44)
C_5	−0.429 33 (85)	−0.128 59 (115)	0.760 90 (58)
C_6	−0.404 41 (91)	−0.238 85 (93)	0.726 04 (69)
C_7	−0.331 54 (94)	−0.222 48 (78)	0.657 87 (72)
C_8	−0.284 87 (69)	−0.094 69 (61)	0.624 17 (52)

[a] The numbers in parentheses are the estimated standard deviations in the last significant digits. [b] Atoms are labeled in agreement with Figure 3.

mass spectra of sufficiently volatile clusters were obtained by using an AEI-MS9 mass spectrometer with a source voltage of 70 eV and probe temperature in the range 100–200 °C. NMR spectra were obtained in either $CDCl_3$, CD_2Cl_2, $CHClF_2$, or toluene-d_8 solutions on a JEOL PS-100 FT Fourier transform NMR spectrometer.

Crystallographic Summary for $H_2FeRu_3(CO)_{12}(PMe_2Ph)$. Pertinent crystal and intensity data are listed in Table II. Complete details of the crystallographic analysis are given in Table A (crystallographic report) of the supplementary material. The structure was solved by direct methods, the four metal atoms were located on an *E* map calculated from a trial set of phases, and the remaining nonhydrogen atoms were located by using standard difference Fourier techniques. The hydrogen atoms, including the two metal hydride ligands, were located by difference Fourier techniques or were placed in their calculated positions (for the PMe_2Ph ligand) and then refined. All nonhydrogen atoms were refined anisotropically, and the hydrogens were refined by using isotropic thermal parameters to give final values of $R_1 = 0.034$ and $R_2 = 0.035$ where

$$R_1 = \sum||F_o| - |F_c||/\sum|F_o| \qquad R_2 = [\sum w(|F_o| - |F_c|)^2/\sum|F_o|^2]^{1/2}$$

Listings of final positional and thermal parameters are given in Tables III–V, and the observed and calculated structure factors are set out in Table B of the supplementary material.

Results

Reaction of $H_2FeRu_3(CO)_{13}$ with Tertiary Phosphines and Phosphites. Mono- and disubstituted derivatives of $H_2FeRu_3(CO)_{13}$ are readily obtained by heating the cluster in the presence of the appropriate phosphine or phosphite ligand, eq 2. In most of the reactions, only mono- and disubstituted

$$H_2FeRu_3(CO)_{13} \xrightarrow[\Delta]{+PR_3,\ -CO} H_2FeRu_3(CO)_{12}(PR_3) + H_2FeRu_3(CO)_{11}(PR_3)_2 \quad (2)$$

$PR_3 = PPh_3$, $PMePh_2$, PMe_2Ph, PMe_3, $P(i\text{-}Pr)_3$, PEt_2Ph, $P(OEt)_2Ph$, $P(OMe)_3$, $P(OEt)_3$

products have been observed, principally because of the nearly 1:1 stoichiometry employed. However, in reactions which utilized excess PPh_3, $P(OEt)_3$, and $P(OMe)_3$, small amounts of material tentatively identified as the respective $H_2FeRu_3(CO)_{10}(PR_3)_3$ derivatives resulted. These substitution reactions appear to proceed cleanly and give only trace amounts of side products unless the reactions are carried out under forcing conditions. A very small amount of a purple compound was detected during chromatography of several of the reaction mixtures, but insufficient amount of this material was isolated to allow characterization. Its purple color, however, is reminiscent of the color of $FeRu_2(CO)_{11}(PMe_2Ph)$[15] and suggests that fragmentation of $H_2FeRu_3(CO)_{13}$ occurs to a small extent to yield substituted $FeRu_2$ trimers. All of the substituted derivatives reported herein are red and are stable in air for prolonged periods. They are all extremely soluble in CH_2Cl_2 but have limited solubility in hexane, and this decreases with increasing PR_3 substitution.

The substituted clusters have been characterized by elemental analysis and by their IR, ^1H and ^{31}P NMR, and mass spectra. One isomer of $H_2FeRu_3(CO)_{12}(PMe_2Ph)$ has been further characterized by a single-crystal X-ray diffraction study. The pertinent spectral data are set out in Tables VI–VIII. The band patterns in the IR spectra of all the substituted clusters are similar to that of the parent $H_2FeRu_3(CO)_{13}$ cluster[3] and thus indicate that no severe structural changes occur upon substitution. The spectra contain IR bands attributable to terminal carbonyls in the 2100–1950-cm^{-1} region in addition to bridging carbonyl bands between 1880 and 1750 cm^{-1}. Increasing phosphine substitution shifts the bands to lower frequency as illustrated by the position of the bridging ν_{CO} bands in the following series (cm^{-1}): $H_2FeRu_3(CO)_{13}$ (1883 w, 1855 m), $H_2FeRu_3(CO)_{12}(P(OMe)_3)$ (1875 w, 1848 m), $H_2FeRu_3(CO)_{11}(P(OMe)_3)_2$ (1862 w, 1812 m), $H_2FeRu_3(CO)_{10}(P(OMe)_3)_3$ (1822 w, 1780 m).

All the clusters have been further characterized by their mass spectra, except for the PPh_3 derivatives, which have insufficient volatility. The spectra generally show a distinct parent ion and ions corresponding to the stepwise loss of all the carbonyl ligands. The mass spectrum of $H_2FeRu_3(CO)_{12}(P(OMe)_3)$, for example, displays a strong parent ion at *m/e* 820 and peaks arising from successive loss of each of the 12 carbonyls. An intense ion at *m/e* 480 is apparent corresponding to the $FeRu_3(P(OMe)_3)$ fragment.

Determination of Ligand Substitution Sites. 1. Monosubstituted Derivatives. The seven distinct positions at which phosphine or phosphite substitution for a carbonyl ligand can occur in $H_2FeRu_3(CO)_{13}$ are indicated by the numbered sites shown in **1**.[16] All the monosubstituted derivatives except

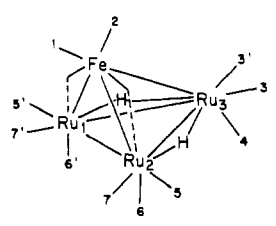

1

(15) Purple $FeRu_2(CO)_{11}(PMe_2Ph)$ can be isolated from the reaction of $FeRu_2(CO)_{12}$ with PMe_2Ph and from the CO-induced fragmentation of $H_2FeRu_3(CO)_{12}(PMe_2Ph)$.[9]

Table IV. Anisotropic Thermal Parameters for Nonhydrogen Atoms in Crystalline $H_2FeRu_3(CO)_{12}(PMe_2Ph)$[a,b]

atom type[c]	B_{11}	B_{22}	B_{33}	B_{12}	B_{13}	B_{23}
Ru_1	2.86 (1)	2.34 (1)	2.38 (1)	0.40 (1)	0.68 (1)	0.27 (1)
Ru_2	4.43 (2)	3.20 (2)	2.45 (1)	0.60 (1)	0.80 (1)	0.05 (1)
Ru_3	3.30 (2)	2.60 (1)	3.26 (2)	0.47 (1)	0.24 (1)	0.51 (1)
Fe	3.03 (3)	3.14 (3)	3.75 (3)	−0.01 (2)	0.64 (2)	0.14 (2)
P	2.98 (5)	3.50 (5)	3.46 (5)	0.65 (4)	0.55 (4)	0.47 (4)
O_{b1}	8.48 (30)	2.85 (16)	10.90 (35)	0.04 (18)	4.35 (27)	−0.20 (19)
O_{b2}	5.28 (21)	5.04 (20)	7.48 (25)	1.29 (16)	2.87 (19)	−0.85 (18)
O_{11}	11.72 (37)	3.05 (17)	5.65 (22)	1.90 (20)	1.85 (23)	1.14 (15)
O_{12}	7.87 (27)	6.80 (24)	4.15 (18)	2.98 (21)	2.45 (18)	−0.44 (17)
O_{21}	6.12 (25)	8.17 (30)	6.35 (25)	0.38 (22)	3.06 (21)	1.11 (21)
O_{22}	14.83 (51)	6.05 (28)	9.48 (36)	4.90 (31)	6.00 (36)	0.10 (25)
O_{23}	8.86 (32)	7.47 (28)	4.51 (21)	−0.19 (24)	−1.91 (21)	0.18 (19)
O_{31}	5.81 (22)	5.82 (22)	5.82 (22)	−0.27 (18)	1.52 (18)	2.34 (18)
O_{32}	12.03 (41)	4.21 (21)	7.02 (27)	2.93 (24)	0.82 (26)	−0.76 (19)
O_{33}	5.90 (24)	8.34 (30)	5.79 (23)	2.10 (22)	−1.54 (19)	1.24 (21)
O_{41}	9.10 (34)	7.47 (29)	6.44 (26)	−0.31 (24)	4.08 (25)	1.77 (22)
O_{42}	4.13 (21)	7.92 (31)	10.73 (38)	0.94 (20)	−1.65 (23)	−1.54 (27)
C_{b1}	4.40 (25)	3.27 (21)	5.60 (28)	0.27 (18)	1.37 (21)	0.49 (19)
C_{b2}	2.85 (19)	3.79 (21)	5.27 (26)	0.56 (16)	0.79 (18)	−0.14 (19)
C_{11}	5.40 (26)	3.12 (19)	3.02 (19)	0.62 (18)	0.83 (18)	−0.05 (15)
C_{12}	4.29 (23)	3.49 (20)	3.60 (20)	1.31 (17)	1.43 (17)	0.40 (16)
C_{21}	5.13 (28)	4.84 (26)	3.43 (21)	0.97 (21)	1.24 (20)	0.55 (18)
C_{22}	7.55 (38)	4.72 (27)	4.10 (25)	1.64 (26)	2.25 (25)	0.03 (21)
C_{23}	6.40 (33)	4.21 (25)	3.65 (23)	−0.34 (22)	0.14 (22)	0.23 (19)
C_{31}	4.15 (23)	4.14 (23)	3.70 (21)	0.22 (18)	0.42 (18)	0.93 (18)
C_{32}	6.52 (33)	3.24 (22)	4.44 (25)	1.03 (21)	0.40 (23)	0.50 (19)
C_{33}	4.39 (25)	4.77 (26)	4.61 (25)	1.24 (21)	0.00 (20)	0.69 (20)
C_{41}	4.68 (27)	4.44 (26)	5.55 (30)	−0.21 (21)	1.46 (23)	0.14 (22)
C_{42}	4.42 (28)	4.48 (26)	5.82 (31)	0.37 (21)	−0.22 (23)	−0.54 (22)
C_1	5.04 (36)	5.93 (38)	8.55 (55)	2.53 (30)	1.71 (37)	0.13 (38)
C_2	4.35 (30)	7.17 (43)	3.98 (26)	−0.11 (30)	−0.63 (22)	1.32 (27)
C_3	2.74 (18)	4.34 (22)	3.89 (21)	0.48 (16)	0.58 (16)	0.54 (17)
C_4	4.58 (29)	6.93 (39)	4.22 (27)	0.26 (27)	1.01 (22)	0.61 (26)
C_5	5.08 (35)	9.60 (61)	5.16 (35)	−1.19 (35)	0.74 (28)	2.86 (37)
C_6	6.07 (40)	5.36 (39)	8.09 (49)	−1.05 (31)	−1.12 (35)	2.54 (36)
C_7	6.79 (42)	4.25 (32)	9.27 (54)	0.03 (29)	0.11 (38)	0.35 (34)
C_8	5.02 (30)	3.71 (24)	7.26 (38)	0.21 (21)	1.80 (27)	0.35 (24)

[a] The numbers in parentheses are the estimated standard deviations in the last significant digits. [b] The anisotropic thermal parameter is of the form $\exp[-0.25(B_{11}h^2a^{*2} + B_{22}k^2b^{*2} + B_{33}l^2c^{*2} + 2B_{12}hka^*b^* + 2B_{13}hla^*c^* + 2B_{23}klb^*c^*)]$. [c] Atoms are labeled in agreement with Figure 3.

Table V. Atomic Coordinates for Hydrogen Atoms in Crystalline $H_2FeRu_3(CO)_{12}(PMe_2Ph)$[a]

atom type[b]	fractional coordinates			isotropic thermal parameter B, Å^2
	x	y	z	
H_1	−0.051 55 (486)	0.317 62 (479)	0.760 82 (318)	3.52 (103)
H_2	−0.005 55 (514)	0.097 81 (495)	0.700 86 (337)	4.03 (112)
H_{11}	−0.307 20 (661)	0.387 96 (706)	0.607 71 (439)	5.76 (153)
H_{12}	−0.310 02 (579)	0.312 20 (554)	0.697 64 (376)	2.88 (128)
H_{13}	−0.450 47 (905)	0.268 28 (790)	0.612 35 (536)	8.77 (207)
H_{21}	−0.268 35 (622)	0.253 46 (636)	0.454 40 (411)	5.36 (136)
H_{22}	−0.408 16 (840)	0.146 41 (736)	0.468 21 (496)	7.50 (189)
H_{23}	−0.274 20 (818)	0.107 69 (792)	0.472 49 (530)	6.86 (240)
H_4	−0.396 63 (544)	0.078 44 (525)	0.750 96 (360)	3.16 (118)
H_5	−0.474 54 (1011)	−0.132 01 (984)	0.800 87 (661)	10.45 (299)
H_6	−0.432 69 (886)	−0.330 23 (926)	0.746 33 (582)	9.68 (237)
H_7	−0.317 95 (966)	−0.307 89 (984)	0.638 45 (642)	10.90 (278)
H_8	−0.231 30 (667)	−0.081 48 (628)	0.571 82 (436)	5.96 (151)

[a] The numbers in parentheses are the estimated standard deviations in the last significant digits. [b] Atoms are labeled in agreement with Figure 3.

$H_2FeRu_3(CO)_{12}(PMe_2Ph)$ and $H_2FeRu_3(CO)_{12}(PMe_3)$, which are discussed separately below, show a temperature-invariant doublet in their ^1H NMR spectra in the δ −17 to −19 region with J_{P-H} = 6–10 Hz (Table II). The corresponding $^{31}P\{^1H\}$ NMR spectra, where obtained, show a temperature-invariant singlet. The magnitude of the P–H coupling constants (6–10 Hz) indicates that in these monosubstituted derivatives the phosphorus is bound to a metal also ligated by hydrogen.[17] This implies substitution on one of the Ru atoms. The only Ru substitution site in which the two hydrogens would be

(16) X-ray crystal structure of $H_2FeRu_3(CO)_{13}$: Gilmore, C. J.; Woodward, P. *J. Chem. Soc. A* **1971**, 3453.

(17) J_{P-H} between phosphorus and hydrogen which do not ligate the same metal is generally less than 3 Hz. For example, in $H_2Os_2Pt_2(CO)_8(PPh_3)_2$, J_{P-H} = 2.5 Hz for coupling between the hydrogens and phosphines located across the cluster[6c] whereas similar distant coupling could not be resolved in $H_4Ru_4(CO)_{10}(Ph_2PCH_2CH_2PPh_2)$.[18] This strongly argues against substitution on the Fe atom.

(18) Shapley, J. R.; Richter, S. I.; Churchill, M. R.; Lashewycz, R. A. *J. Am. Chem. Soc.* **1977**, *99*, 7384.

Table VI. Infrared and NMR Spectral Data for $H_2FeRu_3(CO)_{12}L$ Clusters

L	infrared[a] ν_{CO}, cm^{-1}	NMR, δ ^1H	NMR, δ $^{31}P^b$
PPh_3	2096 m, 2063 s, 2049 s, 2036 sh, 2031 s, 2023 m, 2011 w, 1990 w, 1983 w, 1876 vw, 1849 m	−17.89 d (J_{P-H} = 8.6 Hz)[c]	42.23 s[c]
$PMePh_2$	2097 m, 2074 w, 2063 s, 2048 s, 2031 s, 2021 s, 2012 m, 1987 m, 1878 w, 1850 m, 1806 vw	−17.8 (J_{P-H} = 9.3 Hz)[c]	21.67 s[c]
PMe_2Ph	2096 s, 2072 s, 2064 s, 2046 s, 2034 sh, 2028 s, 2020 s, 2012 m, 1990 m, 1984 m, 1876 w, 1850 m, 1806 m	−18.07 d (J_{P-H} = 10.3 Hz)[d] −18.35 t (J_{P-H} = 1.8 Hz, J_{H-H} = 2.6 Hz) −18.92 dd (J_{P-H} = 9.7 Hz, J_{H-H} = 2.6 Hz)	4.8 s[e] 8.0 s 33.4 s
PMe_3	2097 m, 2073 s, 2064 s, 2047 s, 2037 s, 2030 vs, 2019 m, 2004 w, 1989 w, 1982 w, 1876 w, 1852 w, 1832 w, 1804 m	−18.26 d (J_{P-H} = 11.0 Hz)[f] −18.39 s −19.20 d (J_{P-H} = 9.2 Hz)	
PEt_2Ph	2096 m, 2073 w, 2063 s, 2045 s, 2031 s, 2019 s, 2014 m, 1898 sh, 1984 m, 1876 w, 1850 m, 1806 vw		33.0 s[f]
$P(i\text{-}Pr)_3$	2097 m, 2074 vw, 2064 s, 2044 s, 2032 s, 2018 s, 2014 sh, 1982 m, 1879 w, 1852 m	−18.22 d (J_{P-H} = 6.6 Hz)[c]	
$P(OEt)_2Ph$	2098 m, 2078 m, 2064 s, 2057 s, 2041 m, 2032 s, 2025 s, 2012 m, 1999 m, 1985 sh, 1983 m, 1878 w, 1850 w, 1820 vw	−18.01 d (J_{P-H} = 8.0 Hz)[c]	56.3 s[c]
$P(OMe)_3$	2099 m, 2072 w, 2062 vs, 2052 s, 2024 s, 2015 sh, 1998 m, 1981 m, 1875 w, 1848 m, 1810 vw	−18.53 d (J_{P-H} = 6.1 Hz)[c]	
$P(OEt)_3$	2098 m, 2073 w, 2064 vs, 2052 s, 2031 s, 2025 s, 2013 m, 1996 m, 1983 m, 1876 w, 1848 m	−18.35 d (J_{P-H} = 6.1 Hz)[c]	

[a] Hexane solution. [b] Positive values are downfield from H_3PO_4 as external standard. [c] $CDCl_3$ solution, 27 °C. [d] $CDCl_3$ solution, −50 °C. [e] $CD_2Cl_2/CHClF_2$ solution (2:1), −60 °C. [f] $CDCl_3$ solution, −40 °C.

Table VII. Infrared and NMR Spectral Data for $H_2FeRu_3(CO)_{11}L_2$ Clusters

L	infrared[a] ν_{CO}, cm^{-1}	NMR, δ ^1H	NMR, δ $^{31}P^b$
PPh_3	2077 m, 2058 vw, 2034 vs, 2022 s, 2010 s, 1969 m, 1841 w, 1790 m	−17.12 m, −18.05 m[c] ($J_{H_A-H_B}$ = 1.9 Hz, $J_{H_A-P_A}$ = 10.5 Hz, $J_{H_A-P_B}$ = 2.0 Hz, $J_{H_B-P_A}$ = 6.1 Hz, $J_{H_B-P_B}$ = 6.3 Hz)	41.9 s[c] 36.7 s
PMe_3	2074 m, 2060 vw, 2029 vs, 2019 s, 1999 s, 1964 m, 1840 w, 1781 m	−17.85 m, −18.89 m[d] ($J_{H_A-H_B}$ = 1.9 Hz, $J_{H_A-H_A}$ = 11.8 Hz, $J_{H_A-P_B}$ = 1.3 Hz, $J_{H_B-P_A}$ = 9.6 Hz, $J_{H_B-P_B}$ = 10.5 Hz)	
PEt_2Ph	2077 s, 2065 vw, 2036 s, 2033 s, 2006 s, 1990 vw, 1972 m, 1863 vw, 1792 m[e]		
$P(OMe)_3$	2080 m, 2038 vs, 2029 s, 2009 vs, 1985 m, sh, 1950 m, 1840 w, 1801 m	−1853 m, −18.87 m[f] ($J_{H_A-H_B}$ = 1.9 Hz, $J_{H_A-P_A}$ = 6.3 Hz, $J_{H_A-P_B}$ = 3.2 Hz, $J_{H_B-P_A}$ = 6.0 Hz, $J_{H_B-P_B}$ = 9.2 Hz)	148.7 s[f] 138.5 s
$P(OEt)_2$	2078 m, 2037 vs, 2026 s, sh, 2009 vs, 1946 m, 1839 w, 1789 m	−18.43 m, −18.73 m[d] ($J_{H_A-H_B}$ = 1.9 Hz, $J_{H_A-P_A}$ = 5.5 Hz, $J_{H_A-P_B}$ = 1.7 Hz, $J_{H_B-P_A}$ = 5.4 Hz, $J_{H_B-P_B}$ = 8.6 Hz)	

[a] CH_2Cl_2 solution unless otherwise indicated. [b] Positive shifts are downfield from H_3PO_4 as an external standard. [c] $CDCl_3$ solution, −30 °C. [d] $CDCl_3$ solution, −50 °C. [e] Hexane solution. [f] CD_2Cl_2 solution, −60 °C.

Table VIII. Infrared Spectral Data for $H_2FeRu_3(CO)_{10}L_3$[a]

L	ν_{CO}, cm^{-1}
PPh_3	2060 w, 2044 m, 2026 s, 1996 m, 1979 sh, 1805 w, 1773 m
$P(OMe)_3$	2052 w, 2032 s, 1998 s, 1936 w, 1882 w, 1780 m
$P(OEt)_3$	2051 w, 2031 s, 1993 s, 1979 sh, 1930 w, 1815 sh, 1779 w

[a] CH_2Cl_2 solution.

equivalent and give rise to the doublet in the ^1H NMR spectrum is position 4 in **1**, i.e., axial substitution on the unique Ru. This isomer has a plane of symmetry and is depicted in **2** with its C_s symmetry label.

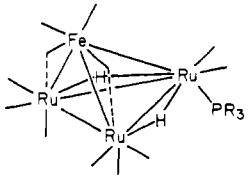

2 (C_s)

The NMR spectra of $H_2FeRu_3(CO)_{12}(PMe_2Ph)$ and $H_2FeRu_3(CO)_{12}(PMe_3)$ are more complex and indicate the presence of substitutional isomers. The $^{31}P\{^1H\}$ NMR spectrum of $H_2FeRu_3(CO)_{12}(PMe_2Ph)$ at −60 °C shows three singlets at δ 33.4, 8.0, and 4.8 with relative intensities 1.0/13.2/7.7. The δ 33.4 resonance is weak and does not change with temperature. It is either a persistent impurity or more likely an isomer in which the phosphine is bound to Fe. The more intense δ 4.8 and 8.0 resonances are attributed to substitutional isomers with phosphine attached to Ru. Significantly, the 27.0 ppm chemical shift difference between the δ 33.4 resonance and the average of the δ 4.8 and δ 8.0 resonances is in the same direction and of the same magnitude as the 26.7 ppm difference in the ^{31}P NMR resonances of $Fe(CO)_3(PPh_3)_2$[19a] (δ 81.8) and $Ru(CO)_3(PPh_3)_2$[19b] (δ 54.9).

The ^1H NMR spectra of $H_2FeRu_3(CO)_{12}(PMe_2Ph)$ and $H_2FeRu_3(CO)_{12}(PMe_3)$ at −50 and −40 °C, respectively, are shown in Figure 1. The intense doublet at δ −18.07 (J_{P-H} =

(19) (a) Clifford, A. J.; Mukherjee, A. K. *Inorg. Synth.* **1966**, *8*, 186. (b) Johnson, B. F. G.; Lewis, J.; Twigg, M. V. *J. Organomet. Chem.* **1974**, *67*, C75.

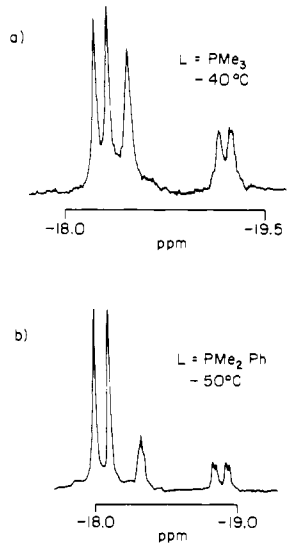

Figure 1. ^1H NMR spectra in $CDCl_3$ solution: (a) $H_2FeRu_3(CO)_{12}(PMe_3)$, −40 °C; (b) $H_2FeRu_3(CO)_{12}(PMe_2Ph)$, −50 °C.

10.3 Hz) in the spectrum of $H_2FeRu_3(CO)_{12}(PMe_2Ph)$ is attributed to the C_s isomer and is analogous to the doublet seen in the ^1H NMR spectra of the derivatives discussed above. The poorly resolved multiplet at δ −18.35 and the doublet of doublets at δ −18.93 (J_{P-H} = 9.7 Hz; J_{H-H} = 2.6 Hz) are of equal intensity and are logically atributed to a second isomer. The magnitude of the P–H coupling constants indicates that in this second isomer, the phosphine ligand is also attached to Ru but not in a position trans to hydride. Shapley and co-workers[18] have provided a definitive example for comparison of cis and trans P–H coupling in an isoelectronic tetranuclear cluster, $H_4Ru_4(CO)_{10}(Ph_2PCH_2CH_2PPh_2)$. In this cluster the hydrogens which are trans to phosphine show J_{P-H} = 28–30 Hz while the cis coupling constants range from 9 to 18 Hz.

In this second isomer, the two hydrogens are clearly nonequivalent. The hydrogen which gives the upfield resonance at δ −18.93 (J_{P-H} = 9.7 Hz) must be bound to the same Ru as the phosphine ligand and in a cis arrangement. For the unresolved multiplet, a P–H coupling constant of 1.8 Hz was determined by computer simulation of the spectrum. This small P–H coupling indicates that the hydrogen is not bound to the same metal as the phosphine but must lie across the cluster. Only substitution at site 5 or 6 in **1** provides these two hydrogen environments. The spectra do not allow a distinction between these sites, although computer simulation of the fluxional processes discussed in the following paper[11] gives results which are more consistent with substitution at site 5. Regardless of whether the phosphine is in site 5 or 6, as shown in **3** and **4**, this isomer is asymmetric and can be denoted by its C_1 symmetry label.

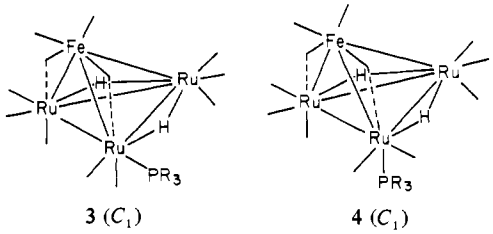

3 (C_1) 4 (C_1)

Integration of the ^1H NMR resonances gives a C_s/C_1 ratio of 4.4/1 for $H_2FeRu_3(CO)_{12}(PMe_2Ph)$. The relative intensities of these resonances indicate that in the $^{31}P\{^1H\}$ NMR spectrum of this derivative (vide supra), the more intense δ 8.0 singlet is due to the C_s isomer while the δ 4.8 resonance is attributed to the C_1 isomer. No hydride resonance attributable to the

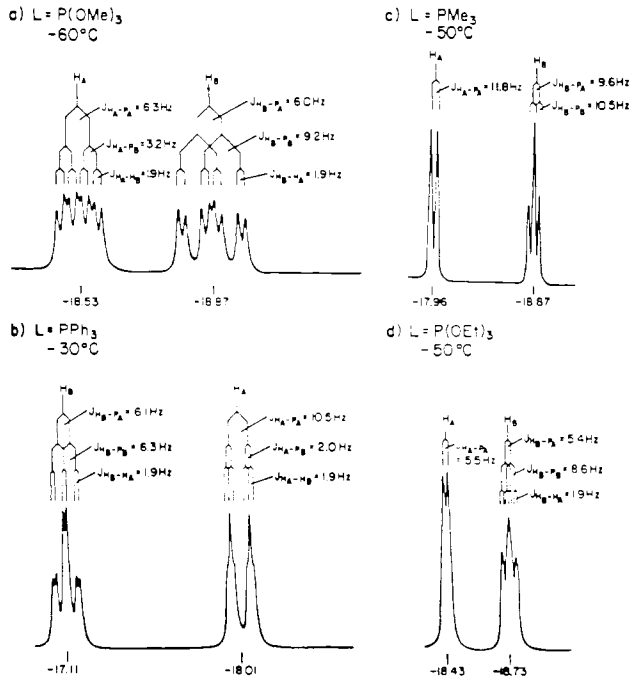

Figure 2. Experimental ^1H NMR spectra with computer-simulated coupling constants: (a) $H_2FeRu_3(CO)_{11}(P(OMe)_3)_2$, CD_2Cl_2, −60 °C; (b) $H_2FeRu_3(CO)_{11}(PPh_3)_2$, $CDCl_3$, −30 °C; (c) $H_2FeRu_3(CO)_{11}(PMe_3)_2$, $CDCl_3$, −50 °C; (d) $H_2FeRu_3(CO)_{11}(P(OEt)_3)_2$, $CDCl_3$, −50 °C.

species which gives the δ 33.4 $^{31}P\{^1H\}$ NMR resonance is apparent in the ^1H NMR spectrum, presumably because of its low relative abundance.

The −40 °C ^1H NMR spectrum of $H_2FeRu_3(CO)_{12}(PMe_3)$, Figure 1, is similar to that of $H_2FeRu_3(CO)_{12}(PMe_2Ph)$ and is fully consistent with the above analysis. The doublet at δ −18.26 (J_{P-H} = 11 Hz) is attributed to the C_s isomer while the δ −19.20 (J_{P-H} = 9.2 Hz) doublet and the δ −18.39 singlet are due to the C_1 isomer. Integration of the ^1H NMR resonances gives a C_s/C_1 ratio of 1.3/1 for $H_2FeRu_3(CO)_{12}(PMe_3)$.

Both $H_2FeRu_3(CO)_{12}(PMe_2Ph)$ and $H_2FeRu_3(CO)_{12}(PMe_3)$ are fluxional as their NMR spectra vary with temperature. These spectra, which demonstrate that the C_s and C_1 isomers undergo rapid interconversion ($k_{20°C} \simeq 500\ s^{-1}$), are discussed in detail in the following article.[11]

2. Disubstituted Derivatives. The experimental low-temperature limiting ^1H NMR spectra for each of the $H_2FeRu_3(CO)_{11}L_2$ (L = PPh_3, PMe_3, $P(OMe)_3$, $P(OEt)_3$) clusters are shown in Figure 2 along with the coupling schemes which have been derived by computer simulation of the spectra. Although qualitatively similar, the particular peak patterns differ for each cluster due to variation in the magnitude of P–H and H–H coupling. The resolution is greatest in the spectrum of $H_2FeRu_3(CO)_{11}(P(OMe)_3)_2$, and it will be discussed in detail.

The $^{31}P\{^1H\}$ NMR spectrum of $H_2FeRu_3(CO)_{11}(P(OMe)_3)_2$ at −60 °C shows a pair of singlets at δ 148.7 and 138.5. As the temperature is raised, these two singlets first coalesce ($T_c \simeq 0$ °C) and then sharpen to a singlet at δ 141.5 at 25 °C. These observations are consistent with the presence of two $P(OMe)_3$ ligands in different environments at the low-temperature limit which then become equivalent at higher temperatures due to fluxional processes occurring in the molecule.[11]

The ^1H NMR spectrum of $H_2FeRu_3(CO)_{11}(P(OMe)_3)_2$ at −60 °C in the metal hydride region, Figure 2, consists of a pair of eight-line multiplets. This spectrum is readily interpreted if it is assumed that substitution occurs such that one phosphite

Table IX. Kinetics of the Reaction of $H_2FeRu_3(CO)_{13}$ with PPh_3[a]

temp, °C	$[PPh_3]$, M	k_{obsd}, s^{-1}
25	5.0×10^{-3}	2.37×10^{-5}
30	5.0×10^{-3}	5.14×10^{-5}
30	1.0×10^{-1}	5.63×10^{-5}
35	5.0×10^{-3}	1.00×10^{-4}
40	2.0×10^{-3}	2.09×10^{-4}
40	5.0×10^{-3}	1.85×10^{-4}
40	5.0×10^{-3}	3.00×10^{-5} [b]
45	5.0×10^{-3}	3.84×10^{-4}
50	5.0×10^{-3}	6.96×10^{-4}
55	5.0×10^{-3}	1.35×10^{-3}

[a] Hexane solution; $[H_2FeRu_3(CO)_{13}] = 1.0 \times 10^{-3}$ M. [b] Under 1 atm CO pressure.

ligand occupies each of the substitution sites which were found for the monosubstituted derivatives. This structure with the appropriate labeling scheme for the magnetically active nuclei is shown in **5**. The multiplets centered at δ −18.53 and −18.87

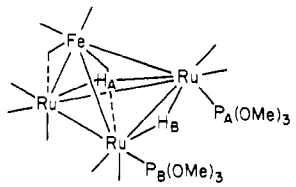

5

are respectively attributed to H_A and H_B, and the appropriate coupling scheme is shown in Figure 2. Computer simulation of the spectrum yielded the following order of coupling constants: $J_{P_B-H_B}$ (9.2 Hz) > $J_{P_A-H_A}$ (6.3 Hz) > $J_{P_A-H_B}$ (6.0 Hz) > $J_{P_B-H_A}$ (3.2 Hz) > $J_{H_A-H_B}$ (1.9 Hz).

Selective decoupling of the ^{31}P NMR resonances confirms the above assignments although H–H coupling could not be resolved in these experiments. Decoupling of the δ 148.7 ^{31}P NMR resonance causes the ^1H NMR spectrum to collapse into a doublet for H_B ($J_{P_B-H_B}$ = 9.2 Hz) and a broad singlet for H_A. Thus, the δ 148.7 ^{31}P NMR resonance is attributed to P_A. Decoupling of the δ 138.5 ^{31}P NMR resonance attributable to P_B yields a doublet for H_B ($J_{P_A-H_B}$ = 5.6 Hz) and a doublet for H_A ($J_{P_A-H_A}$ = 6.7 Hz). Decoupling of either P_A or P_B yields a doublet for H_B because it is still split strongly by the other phosphorus atom, to which it is also cis.

The low-temperature ^1H NMR spectra of the other disubstituted derivatives can be similarly assigned, although the relative magnitudes of the coupling constants vary and consequently have a profound effect on the resonance patterns as illustrated in Figure 2. The specific coupling constants that were extracted from computer simulation of the spectra assuming the basic structure shown in **5** are set out in Figure 2 and listed in Table VII. One curious feature is the reversal of relative positioning of the hydride resonances for the PPh_3 derivative compared to those of the other disubstituted clusters. For $H_2FeRu_3(CO)_{11}(PPh_3)_2$, the observed ordering δ_{H_A} (−18.01 ppm) < δ_{H_B} (−17.11 ppm) is opposite to that of the other derivatives.

Kinetics of the Reaction of $H_2FeRu_3(CO)_{13}$ with PPh_3. In an attempt to understand the mechanism by which these substitution reactions proceed, a kinetic study of the reaction of PPh_3 with $H_2FeRu_3(CO)_{13}$ was undertaken. The rate of disappearance of $H_2FeRu_3(CO)_{13}$ over a 25–55 °C temperature range was monitored by analytical liquid chromatography. First-order rate plots obtained by using chromatographic peak areas were linear to 80% completion. An Arrhenius plot of the k_{obsd} values set out in Table IX gave a straight line and afforded the activation parameters $\Delta H°‡$ = 25.3 ± 0.9 kcal/mol and $\Delta S°‡$ = 4.9 ± 3.1 cal/(mol K). For determination of the reaction order with respect to phosphine, the concentration of PPh_3 was varied from a 2-fold to a 100-fold excess. The k_{obsd} values for these experiments at 30 and 40 °C are set out in Table IX. When the reaction of $H_2FeRu_3(CO)_{13}$ with PPh_3 was carried out at 40 °C under an atmosphere of CO, the rate was roughly 6 times slower than it was under N_2.

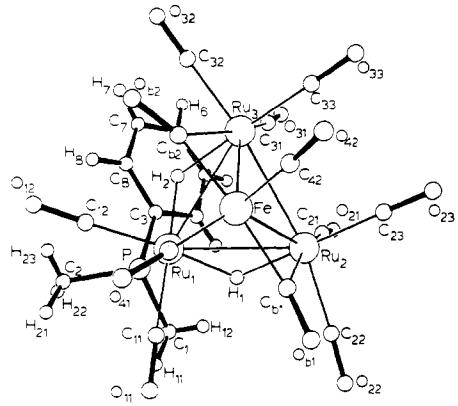

Figure 3. A perspective drawing, adapted from an ORTEP plot, of the solid-state structure of $H_2FeRu_3(CO)_{12}(PMe_2Ph)$. For the purpose of clarity, all atoms are represented by open circles which are in no way representative of their true thermal motion.

Table X. Selected Bond Lengths (Å) in Crystalline $H_2FeRu_3(CO)_{12}(PMe_2Ph)$[a,b]

Ru_1–Ru_2	2.910 (1)	Ru_1–Fe	2.720 (1)
Ru_1–Ru_3	2.923 (1)	Ru_2–Fe	2.721 (1)
Ru_2–Ru_3	2.823 (1)	Ru_3–Fe	2.692 (1)
Ru_1–P	2.326 (1)		
Ru_1–C_{11}	1.875 (5)	Fe–C_{41}	1.775 (6)
Ru_1–C_{12}	1.888 (5)	Fe–C_{42}	1.794 (7)
Ru_2–C_{21}	1.888 (6)		
Ru_2–C_{22}	1.918 (7)	Ru_2–C_{b1}	2.368 (6)
Ru_2–C_{23}	1.914 (6)	Ru_3–C_{b2}	2.312 (6)
Ru_3–C_{31}	1.903 (6)		
Ru_3–C_{32}	1.930 (6)	Fe–C_{b1}	1.822 (6)
Ru_3–C_{33}	1.908 (6)	Fe–C_{b2}	1.830 (5)
O_{11}–C_{11}	1.137 (6)	O_{32}–C_{32}	1.124 (8)
O_{12}–C_{12}	1.133 (7)	O_{33}–C_{33}	1.127 (8)
O_{21}–C_{21}	1.141 (8)	O_{41}–C_{41}	1.136 (8)
O_{22}–C_{22}	1.125 (9)	O_{42}–C_{42}	1.133 (9)
O_{23}–C_{23}	1.134 (8)	O_{b1}–C_{b1}	1.161 (7)
O_{31}–C_{31}	1.139 (7)	O_{b2}–C_{b2}	1.168 (7)
P–C_1	1.801 (9)	P–C_3	1.821 (5)
P–C_2	1.814 (7)		
Ru_1–H_1	1.80 (5)	Ru_2–H_1	1.79 (5)
Ru_1–H_2	1.72 (5)	Ru_3–H_2	1.81 (5)

[a] The numbers in parentheses are the estimated standard deviations in the last significant digits. [b] Atoms are labeled in agreement with Figure 3.

Crystal and Molecular Structure of the C_s Isomer of $H_2FeRu_3(CO)_{12}(PMe_2Ph)$. Crystals of $H_2FeRu_3(CO)_{12}(PMe_2Ph)$ can be isolated by slow evaporation of solvent from a hexane solution of the cluster. An arbitrary single crystal was chosen and subjected to a complete structural analysis by X-ray diffraction. The determined structure is depicted in Figure 3 and is clearly that of the C_s isomer. We do not know whether this isomer preferentially crystallizes from hexane solution or whether a crystal of this isomer was by chance chosen from a mixture of C_s and C_1 crystals. All the crystals appeared similar upon microscopic examination.

Relevant bond lengths and angles for $H_2FeRu_3(CO)_{12}(PMe_2Ph)$ are set out in Tables X and XI. The overall geometry of this isomer of $H_2FeRu_3(CO)_{12}(PMe_2Ph)$ is quite similar to that of the parent $H_2FeRu_3(CO)_{13}$ cluster,[16] implying that little distortion occurs upon PR_3 substitution, at

Table XI. Selected Bond Angles (Deg) in Crystalline $H_2FeRu_3(CO)_{12}(PMe_2Ph)$[a,b]

$Ru_2Ru_1Ru_3$	57.91 (1)	$Ru_1Ru_3Ru_2$	60.81 (1)
Ru_2Ru_1Fe	57.69 (2)	Ru_1Ru_3Fe	57.78 (2)
Ru_3Ru_1Fe	56.86 (2)	Ru_2Ru_3Fe	59.07 (2)
$Ru_1Ru_2Ru_3$	61.28 (1)	Ru_1FeRu_2	64.65 (2)
Ru_1Ru_2Fe	57.65 (2)	Ru_1FeRu_3	65.36 (2)
Ru_3Ru_2Fe	58.06 (2)	Ru_2FeRu_3	62.87 (2)
$Ru_2C_{b1}Fe$	79.8 (2)	$Ru_3C_{b2}O_{b2}$	128.0 (4)
$Ru_3C_{b2}Fe$	80.2 (2)	$FeC_{b1}O_{b1}$	154.1 (5)
$Ru_2C_{b1}O_{b1}$	126.0 (5)	$FeC_{b2}O_{b2}$	151.8 (5)
PRu_1C_{11}	92.8 (2)	PRu_1Ru_3	112.25 (3)
PRu_1C_{12}	92.2 (2)	PRu_1Ru_2	110.59 (4)
PRu_1Fe	166.5 (4)		
$Ru_1C_{11}O_{11}$	177.7 (5)	$Ru_3C_{31}O_{31}$	174.6 (5)
$Ru_1C_{12}O_{12}$	177.9 (5)	$Ru_3C_{32}O_{32}$	179.0 (6)
$Ru_2C_{21}O_{21}$	174.3 (5)	$Ru_3C_{33}O_{33}$	178.8 (6)
$Ru_2C_{22}O_{22}$	177.2 (6)	$FeC_{41}O_{41}$	177.8 (6)
$Ru_2C_{23}O_{23}$	178.3 (6)	$FeC_{42}O_{42}$	175.8 (6)
$Ru_2Ru_1H_1$	36 (2)	$Ru_3Ru_1H_2$	35 (2)
$Ru_1Ru_2H_1$	36 (2)	$Ru_1Ru_3H_2$	33 (2)
$Ru_1H_1Ru_2$	108 (2)	$Ru_1H_2Ru_3$	112 (3)

[a] The numbers in parentheses are the estimated standard deviations in the last significant digits. [b] Atoms are labeled in agreement with Figure 3.

least when substitution occurs to give the C_s isomer. As in $H_2FeRu_3(CO)_{13}$, four carbonyls are bound to the Fe atom, with two of these asymmetrically bridging Fe–Ru bonds. For these latter carbonyls, the average Fe–C_b distance (1.785 Å) compares well with the corresponding distance in $H_2FeRu_3(CO)_{13}$ (Fe–C_b(av) = 1.78 Å) although the Ru–C_b distances (average 2.340 Å) average 0.06 Å longer than those of $H_2FeRu_3(CO)_{13}$ (Ru–C_b(av) = 2.28 Å).

The hydride ligands were not located in the $H_2FeRu_3(CO)_{13}$ structure[16] but their positions were inferred from the relative lengths of the Ru–Ru vectors: average Ru–Ru(H bridged) = 2.91 Å; average Ru–Ru(unbridged) = 2.80 Å. The hydride ligands have been located and refined in the $H_2FeRu_3(CO)_{12}(PMe_2Ph)$ structure, Figure 3, and the Ru–Ru bond lengths compare reasonably well to the corresponding lengths in $H_2FeRu_3(CO)_{13}$: average Ru–Ru(H bridged) = 2.917 Å; Ru–Ru(unbridged) = 2.823 Å. The phosphorus atom lies 2.11 Å below the Ru_3 plane and on the pseudo-mirror plane defined by Fe, Ru_2, and the midpoint of the Ru_2–Ru_3 bond.

Discussion

Substitution Sites. The low symmetries of the substituted $H_2FeRu_3(CO)_{13-x}L_x$ derivatives discussed herein has allowed the use of ^1H NMR spectroscopy to assign the specific substitution sites which the ligands L occupy. As shown above, the monosubstituted derivatives can exist in two isomeric forms of C_s (**2**) and C_1 (**3**) symmetries and the disubstituted derivatives adopt structure **5**. Kaesz and Koepke[20] have studied $P(OMe)_3$-substituted derivatives of $H_2Ru_4(CO)_{13}$,[21] which is isostructural with $H_2FeRu_3(CO)_{13}$, **1**, and their results are fully consistent with those reported herein. Three isomers of $H_2Ru_4(CO)_{12}(P(OMe)_3)$ were observed, two of which are directly analogous to the C_s and C_1 isomers of the $H_2FeRu_3(CO)_{12}(PR_3)$ clusters. The third isomer has a $P(OMe)_3$ ligand substituted on the Ru atom that is ligated by the two semibridging CO's (similar to the Fe atom in $H_2FeRu_3(CO)_{13}$, **1**). The ^{31}P NMR spectrum of $H_2FeRu_3(CO)_{12}(PMe_2Ph)$ discussed above suggests the presence of such an isomer of this derivative, but its very low abundance has not allowed a definitive assignment. Two isomers of the disubstituted $H_2Ru_4(CO)_{11}(P(OMe)_3)_2$ derivative were observed by Kaesz and Koepke,[20] one of which is directly analogous to structure **5** for $H_2FeRu_3(CO)_{11}(P(OMe)_3)_2$. Again, the second isomer of $H_2Ru_4(CO)_{11}(P(OMe)_3)_2$ possesses a $P(OMe)_3$ ligand on the Ru atom ligated by the two semibridging carbonyls, but not evidence for such an isomer was obtained for the $H_2FeRu_3(CO)_{11}L_2$ derivatives. There is thus an obvious strong preference for PR_3 substitution on the Ru atoms of $H_2FeRu_3(CO)_{12}$ rather than Fe. Since the structures of $H_2Ru_4(CO)_{13}$[21] and $H_2FeRu_3(CO)_{13}$[16] are so similar, it is doubtful that steric reasons alone can account for the lack of Fe-substituted derivatives of the latter and hence electronic factors must be important.

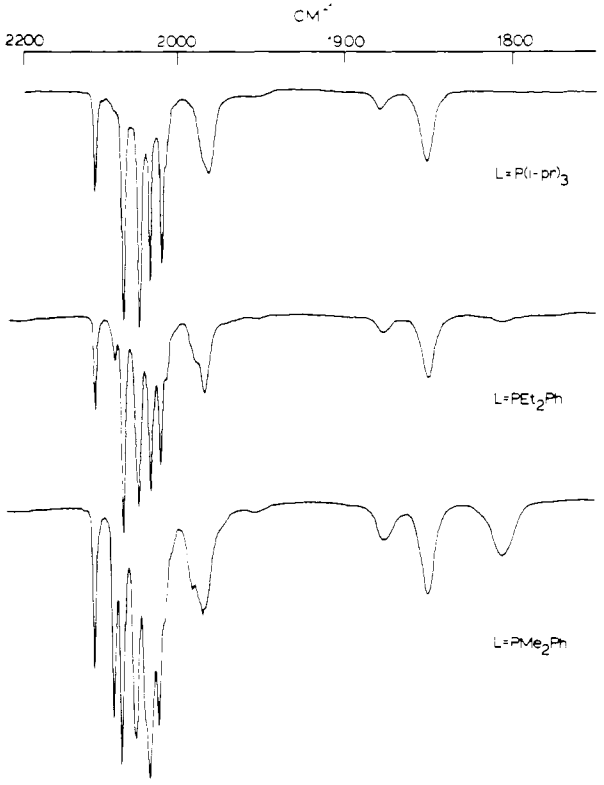

Figure 4. Infrared spectra of $H_2FeRu_3(CO)_{11}L$ (L = P(*i*-Pr)$_3$, PEt_2Ph, PMe_2Ph) in hexane solution.

Influence of Ligand Size and Basicity on Substitution Site Preference. Although the ^1H NMR spectra allow a determination of the specific substitution sites which the ligands L occupy in the monosubstituted $H_2FeRu_3(CO)_{12}L$ derivatives, the IR spectra of these derivatives in hexane solution have proven to be a more convenient indicator of the existence of isomers and their relative ratios. For example, the IR spectrum of $H_2FeRu_3(CO)_{12}(PMe_2Ph)$, Figure 4, shows two extra bands at 2072 and 1806 cm^{-1}, which are not seen in the spectrum of $H_2FeRu_3(CO)_{12}(P(i\text{-}Pr)_3)$ which appears to exist solely as the C_s isomer. These two extra bands are attributed to the less abundant C_1 isomer of $H_2FeRu_3(CO)_{12}(PMe_2Ph)$. Similar bands are seen in the spectra of the other derivatives, Table VI, although their relative intensities vary with the C_s/C_1 ratio.

A comparison of the relative intensities of the ~1806-cm^{-1} (C_1) and the ~1850-cm^{-1} (C_s) bridging carbonyl bands allows a qualitative estimation of the relative abundance of the C_s and C_1 isomers of each derivative.[22] The C_s/C_1 ratios can

(20) (a) Koepke, J. W. Ph.D. Dissertation, University of California, Los Angeles, 1974. (b) Kaesz, H. D. In "Organotransition-Metal Chemistry"; Ishii, Y., Tsutsui, M., Eds.; Plenum Press: New York, 1975; p 291.

(21) Yawney, D. B. W.; Doedens, R. J. *Inorg. Chem.* **1972**, *11*, 838.

(22) This analysis assumes similar extinction coefficients for the bands of the two isomers. If the ϵ's differ markedly, the values of $K_{C_1 \rightleftarrows C_s}$ given in Table XII will be in error; however, the conclusions drawn from the relative values will still be valid.

Table XII. Effect of Ligand Size and Basicity on the $C_1 \rightleftarrows C_s$ Equilibrium

ligand	cone angle,[a] deg	basicity,[b] cm^{-1}	K^c
$P(i\text{-}Pr)_3$	160	2059.2	>100
PPh_3	145	2068.9	>100
$PMePh_2$	136	2067.0	11
PEt_2Ph	136	2063.7	11
$P(OMe)_3$	107	2079.5	10
$P(OEt)_2Ph$	116	2074.2	5.5
PMe_2Ph	122	2065.3	1.8
PMe_3	118	2064.1	0.4

[a] Reference 23. [b] The more basic the phosphorus donor ligand is, the lower the C-O stretching frequency. See ref 23. [c] Calculated for the $C_1 \rightleftarrows C_s$ equilibrium, estimated from the ratio of the peak height of the ~1850-cm^{-1} band to that of the ~1806-cm^{-1} band of the spectra measured in hexane solution.

be correlated with the size and basicity of the ligand by using data tabulated by Tolman,[23] Table XII. As can be seen by inspection of Table XII, no correlation can be made by using ligand size or basicity alone, and both factors govern the choice of substitution site. With large ligands such as $P(i\text{-}Pr)_3$ and PPh_3, the steric bulk of the ligand determines the site of substitution. Substitution is limited to give the C_s isomer, regardless of ligand basicity. These two ligands differ markedly in basicity with $P(i\text{-}Pr)_3$ (2059.2 cm^{-1}) being the most basic of all the ligands examined whereas PPh_3 (2068.9 cm^{-1}) is among the least basic. Conversely, for smaller ligands basicity becomes the controlling factor, and the C_1 isomer becomes more abundant as the basicity of the ligand increases. This effect is best illustrated by comparing the ligands PMe_3 and $P(OMe)_3$. The former is highly basic, and in hexane solution it gives a $C_1 \rightleftarrows C_s$ equilibrium constant of 0.4, whereas the smaller but less basic $P(OMe)_3$ gives $K_{C_1 \rightleftarrows C_s} = 10$.[24]

The C_s isomer is preferred for large ligands presumably because there is less steric hindrance in this substitution site. Analysis of the structural data for $H_2FeRu_3(CO)_{13}$, as determined by Gilmore and Woodward,[16] does not indicate that the carbonyl occupying position 4 in **1** (C_s) is less crowded than any of the other carbonyls. However, there is more freedom in arranging the ligands bound to this unique Ru atom than there is for the ligands bound to Ru_1 or Ru_2 because of the additional constraints on the latter imposed by the bridging carbonyls. Thus Ru_3 can better accommodate a large ligand than can Ru_1 or Ru_2. The determined structure of the C_s isomer of $H_2FeRu_3(CO)_{12}(PMe_2Ph)$, Figure 3, certainly does not indicate that the presence of the PMe_2Ph ligand has any significant consequences on the overall cluster geometry compared to the case for $H_2FeRu_3(CO)_{13}$.

The increased abundance of the C_1 isomer with increased ligand basicity may reflect the ability of the bridging carbonyl to delocalize electron density from the substituted metal in this isomer. The increased downfield chemical shift of one of the bridging carbonyls in the ^{13}C NMR spectrum of $H_2FeRu_3(CO)_{12}(PMe_2Ph)$ (249 ppm)[11] compared to that of $H_2FeRu_3(CO)_{13}$ (229 ppm)[9] implies a shift from semibridging to more nearly full bridging,[9,25-27] and the shift to lower energy of the bridging carbonyl infrared absorption in the C_1 isomers

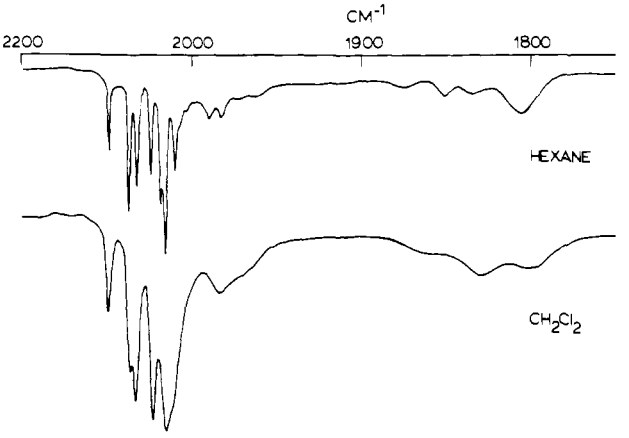

Figure 5. Infrared spectra of $H_2FeRu_3(CO)_{12}(PMe_3)$ in CH_2Cl_2 and hexane solution.

(~1806 cm^{-1} vs. ~1850 cm^{-1} for the C_s isomers) supports this contention.

As illustrated in Figure 5, the $C_s \rightleftarrows C_1$ equilibrium is dramatically solvent dependent, with the polar CH_2Cl_2 solvent shifting the $H_2FeRu_3(CO)_{12}(PMe_3)$ equilibrium in the direction of the C_s isomer. Polar solvents such as CH_2Cl_2 can stabilize the increased electron density on the substituted metal in the C_s isomer and thereby diminish the need to convert to the C_1 isomer. The failure to observe any evidence for the C_1 isomer in the ^1H NMR spectra of most of the monosubstituted derivatives is presumably due to the recording of these spectra in polar $CDCl_3$, CD_2Cl_2, and $CHCl_2F$ solvents, necessitated by the limited solubility of these compounds in nonpolar solvents.

Kinetics of the Reaction of $H_2FeRu_3(CO)_{13}$ with PPh_3. Mechanistic Implications. The kinetic data suggest that the reaction of $H_2FeRu_3(CO)_{13}$ with PPh_3 is first order with respect to cluster and zero order with respect to phosphine (eq 3). The zero-order dependence on PPh_3, the positive value

$$-d[H_2FeRu_3(CO)_{13}]/dt = k_1[H_2FeRu_3(CO)_{13}] \quad (3)$$

of $\Delta S^{\circ\ddagger}$ (+4.9 cal/(mol K)), and the decrease in the reaction rate under a CO atmosphere all argue for a dissociative mechanism in which the rate-determining step is loss of CO from $H_2FeRu_3(CO)_{13}$ (eq 4). This generates an unsaturated $H_2FeRu_3(CO)_{12}$ intermediate, which can rapidly add PPh_3 to give the monosubstituted derivative (eq 5).

$$H_2FeRu_3(CO)_{13} \underset{k_2}{\overset{k_1\ (slow)}{\rightleftharpoons}} H_2FeRu_3(CO)_{12} + CO \quad (4)$$

$$H_2FeRu_3(CO)_{12} + PPh_3 \xrightarrow[fast]{k_3} H_2FeRu_3(CO)_{12}(PPh_3) \quad (5)$$

Although a detailed kinetic study of the formation of the disubstituted derivative was not undertaken, it became evident through the course of this work that the monosubstituted $H_2FeRu_3(CO)_{12}(PPh_3)$ cluster reacts 2–3 times more rapidly with PPh_3 than does $H_2FeRu_3(CO)_{13}$. Similar behavior has been reported for the reaction of $Ir_4(CO)_{12}$ with PPh_3, although there the rate difference is far greater.[28] However, the disubstituted $H_2FeRu_3(CO)_{11}(PPh_3)_2$ cluster reacts extremely slowly with PPh_3, in contrast to the situation found for $Ir_4(CO)_{10}(PPh_3)_2$,[28] and it was necessary to carry out this reaction in toluene for 12 h at 70 °C in order to obtain an appreciable conversion to the trisubstituted derivative.

Kinetic studies employing the smaller but more basic $P(OMe)_3$ as the entering ligand did not give as straightforward results as those with PPh_3. Although the experiments with

(23) Tolman, C. A. *Chem. Rev.* **1977**, *77*, 313.
(24) The variable-temperature NMR data discussed in the following article[11] indicate that the C_1 and C_s isomers rapidly interconvert on the ^1H NMR time scale at 25 °C and thus a true $C_1 \rightleftarrows C_s$ equilibrium is obtained in these solutions.
(25) Evans, J.; Johnson, B. F. G.; Lewis, J.; Norton, J. R.; Cotton, F. A. *J. Chem. Soc., Chem. Commun.* **1973**, 807.
(26) Johnson, B. F. G.; Lewis, J.; Matheson, T. W. *J. Chem. Soc., Chem. Commun.* **1974**, 441.
(27) Stuntz, G. F.; Shapley, J. R. *J. Am. Chem. Soc.* **1977**, *99*, 607.
(28) Karel, K. R.; Norton, J. R. *J. Am. Chem. Soc.* **1974**, *96*, 6812.

$P(OMe)_3$ suggested a nonzero dependence on phosphite concentration, we were not able to fit our data to any reasonable rate equation. Similar nonzero dependence on phosphite concentration has been observed previously in substitution reactions of $Ru_3(CO)_{12}$[29] and $Co_4(CO)_{12}$.[30]

Summary

Although the field of metal cluster chemistry has been growing at a very rapid rate, a need still exists for fundamental reactivity studies of cluster systems. In this work, a series of phosphine- and phosphite-substituted derivatives of $H_2FeRu_3(CO)_{13}$ has been prepared and characterized. A kinetic study of the reaction of $H_2FeRu_3(CO)_{13}$ with PPh_3 has revealed that the substitution reaction proceeds via a [PPh_3]-independent pathway, presumably involving CO dissociation in the rate-determing step producing an unsaturated $H_2FeRu_3(CO)_{12}$ intermediate.

^1H and ^{31}P NMR spectra have further shown that the monosubstituted clusters exist in two isomeric forms of C_s and C_1 symmetries, each of which has the phosphorus ligand bound to a Ru atom. The C_s/C_1 isomer ratio is dependent on ligand size, ligand basicity, and the solvent employed. Large ligands, regardless of basicity, give only the C_s isomer. With smaller ligands, basicity becomes the controlling factor, with the more basic ligands preferring the C_1 isomer. The disubstituted $H_2FeRu_3(CO)_{11}L_2$ clusters possess a phosphine or phosphite ligand in each of the substitution sites established for the monosubstituted derivatives.

The fluxional properties of the substituted clusters, in which the phosphines exchange substitution sites by an intramolecular process involving a subtle rearrangement of the cluster framework, and the reactions of $H_2FeRu_3(CO)_{13}$ with alkynes are discussed in the following two papers.[11,12]

Acknowledgment. This work was supported in part by the Office of Naval Research. We thank A. Freyer and R. Minard for assistance in obtaining the NMR and mass spectra and the National Science Foundation's major equipment grant program for providing matching funds to purchase the JEOL 100-FT and Bruker WH 200 NMR spectrometers and the AEI MS-902 mass spectrometer. G.L.G. and V.W.D. gratefully acknowledge the Camille and Henry Dreyfus Foundation for Teacher-Scholar awards, and G.L.G. thanks the Alfred P. Sloan Foundation for a research fellowship.

Registry No. $H_2FeRu_3(CO)_{13}$, 32036-04-7; $H_2FeRu_3(CO)_{12}(PPh_3)$, 74128-12-4; $H_2FeRu_3(CO)_{11}(PPh_3)_2$, 78248-92-7; $H_2FeRu_3(CO)_{10}(PPh_3)_3$, 78249-48-6; $H_2FeRu_3(CO)_{12}(PMePh_2)$ (C_s isomer), 78249-49-7; $H_2FeRu_3(CO)_{12}(PMePh_2)$ (C_1 isomer), 78249-50-0; $H_2FeRu_3(CO)_{12}(PMe_2Ph)$ (C_s isomer), 78128-11-3; $H_2FeRu_3(CO)_{12}(PMe_2Ph)$ (C_1 isomer), 78128-07-7; $H_2FeRu_3(CO)_{12}(PMe_3)$ (C_s isomer), 78248-89-2; $H_2FeRu_3(CO)_{12}(PMe_3)$ (C_1 isomer), 78248-90-5; $H_2FeRu_3(CO)_{11}(PMe_3)_2$, 78249-51-1; $H_2FeRu_3(CO)_{12}(P(i\text{-}Pr)_3)$, 78249-52-2; $H_2FeRu_3(CO)_{12}(PEt_2Ph)$ (C_s isomer), 78249-53-3; $H_2FeRu_3(CO)_{12}(PEt_2Ph)$ (C_1 isomer), 78249-54-4; $H_2FeRu_3(CO)_{11}(PEt_2Ph)_2$, 78265-04-0; $H_2FeRu_3(CO)_{12}(P(OEt)_2Ph)$ (C_s isomer), 78265-06-2; $H_2FeRu_3(CO)_{12}(P(OEt)_2Ph)$ (C_1 isomer), 78249-55-5; $H_2FeRu_3(CO)_{12}(P(OMe)_3)$ (C_s isomer), 78265-85-7; $H_2FeRu_3(CO)_{12}(P(OMe)_3)$ (C_1 isomer), 78249-56-6; $H_2FeRu_3(CO)_{11}(P(OMe)_3)_2$, 78248-91-6; $H_2FeRu_3(CO)_{10}(P(OMe)_3)_3$, 78265-86-8; $H_2FeRu_3(CO)_{12}(P(OEt)_3)$ (C_s isomer), 78249-57-7; $H_2FeRu_3(CO)_{12}(P(OEt)_3)$ (C_1 isomer), 78249-58-8; $H_2FeRu_3(CO)_{11}(P(OEt)_3)_2$, 78248-86-9; $H_2FeRu_3(CO)_{10}(P(OEt)_3)_3$, 78248-87-0; PPh_3, 603-35-0.

Supplementary Material Available: Table A (crystal structure analysis report) and Table B (structure factor amplitudes) (30 pages). Ordering information is given on any current masthead page.

(29) (a) Poë, A. J.; Twigg, M. V. *J. Organomet. Chem.* **1973**, *50*, C39. (b) Poë, A. J.; Twigg, M. V. *J. Chem. Soc., Dalton Trans.* **1974**, 1860.
(30) Darensbourg, D. J.; Incorvia, M. J. *J. Organomet. Chem.* **1979**, *171*, 89.

Contribution from the Department of Chemistry,
The Pennsylvania State University, University Park, Pennsylvania 16802

Ligand Site Exchange Induced by Intrametallic Rearrangement Processes in $H_2FeRu_3(CO)_{13-x}(PR_3)_x$ (x = 1, 2)

WAYNE L. GLADFELTER, JOSEPH R. FOX, JOHN A. SMEGAL, TIMOTHY G. WOOD, and GREGORY L. GEOFFROY*

Received January 27, 1981

The fluxional processes which occur in $H_2FeRu_3(CO)_{12}L$ (L = PMe_2Ph, PMe_3) and $H_2FeRu_3(CO)_{11}L_2$ (L = PMe_3, PPh_3, $P(OMe)_3$, $P(OEt)_3$) have been studied by a combination of variable-temperature ^1H, ^{31}P, and ^{13}C NMR spectroscopy. The fluxional processes are basically the same as those which have been shown to occur in the unsubstituted $H_2FeRu_3(CO)_{13}$ cluster and involve bridge–terminal CO exchange localized on Fe, cyclic exchange of the carbonyls about the triangular face of the cluster which possesses the bridging CO's, and rearrangement of the metal framework with a corresponding shift of the hydrides and carbonyls. The intrametallic rearrangement process is of profound importance in these substituted derivatives since it leads to exchange of the substitution sites. For the monosubstituted derivatives, this exchange leads to the facile $C_s \rightleftarrows C_1$ isomerization observed, and for the disubstituted derivative it renders the phosphorus donor ligands equivalent on the time scale of the NMR measurements.

We have previously reported that the mixed-metal clusters $H_2FeRu_3(CO)_{13}$, $H_2FeRu_2Os(CO)_{13}$, and $H_2FeRuOs_2(CO)_{13}$ undergo a variety of fluxional processes including one that involves a subtle shift in the metal framework, as illustrated in (1) for the $C_1 \rightleftarrows C_s$ isomerization of $H_2FeRuOs_2(CO)_{13}$.[1,2] The mono- and disubstituted $H_2FeRu_3(CO)_{13-x}L_x$ clusters, in which L is a tertiary phosphine or phosphite and whose preparation was described in the preceding paper,[3] are also

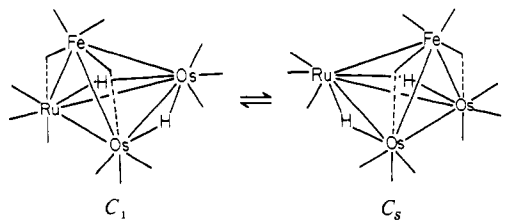

C_1 C_s (1)

fluxional and undergo a similar intrametallic rearrangement process. *This process is of critical importance for these substituted derivatives since it interchanges the two substitution sites which the ligands L occupy.* For the monosub-

(1) Geoffroy, G. L.; Gladfelter, W. L. *J. Am. Chem. Soc.* **1977**, *99*, 6775.
(2) Gladfelter, W. L.; Geoffroy, G. L. *Inorg. Chem.* **1980**, *19*, 2579.
(3) Fox, J. R.; Gladfelter, W. L.; Wood, T. G.; Smegal, J. A.; Foreman, T. K.; Geoffroy, G. L. *Inorg. Chem.*, companion paper in this issue.

0020-1669/81/1320-3223$01.25/0